Pharm Res (2020) 37: 195
https://doi.org/10.1007/s11095-020-02925-6

RESEARCH PAPER

Design of Chitosan Nanocapsules with Compritol 888 ATO® for Imiquimod Transdermal Administration. Evaluation of Their Skin Absorption by Raman Microscopy

María Javiera Alvarez-Figueroa[1] • Daniela Narváez-Araya[1] • Nicolás Armijo-Escalona[1] • Eduardo A. Carrasco-Flores[2] • José Vicente González-Aramundiz[1,3]

Received: 20 May 2020 / Accepted: 7 September 2020 / Published online: 17 September 2020

ABSTRACT

Purpose Design imiquimod-loaded chitosan nanocapsules for transdermal delivery and evaluate the depth of imiquimod transdermal absorption as well as the kinetics of this absorption using Raman Microscopy, an innovative strategy to evaluate transdermal absorption. This nanovehicle included Compritol 888ATO®, a novel excipient for formulating nanosystems whose administration through the skin has not been studied until now.

Methods Nanocapsules were made by solvent displacement method and their physicochemical properties was measured by DLS and laser-Doppler. For transdermal experiments, newborn pig skin was used. The Raman spectra were obtained using a laser excitation source at 532 nm and a 20/50X oil immersion objective.

Results The designed nanocapsules, presented nanometric size (180 nm), a polydispersity index <0.2 and a zeta potential +17. The controlled release effect of Compritol was observed, with the finding that half of the drug was released at 24 h in comparison with control ($p < 0.05$). It was verified through Raman microscopy that imiquimod transdermal penetration is dynamic, the nanocapsules take around 50 min to penetrate the stratum corneum and 24 h after transdermal administration, the drug was in the inner layers of the skin.

Conclusions This study demonstrated the utility of Raman Microscopy to evaluate the drugs transdermal penetration of in the different layers of the skin.

KEY WORDS chitosan-nanocapsules · compritol 888 ATO® · imiquimod · Raman microscopy · transdermal

INTRODUCTION

Transdermal admistration has many advantages over oral administration, such as reduce first-pass metabolism and decrease adverse effects, providing a dosing regimen that decreases inter- and intra-patient variability, etc. (1). However, since the function of the skin is to be a protective barrier, its outermost layer, the stratum corneum, restricts the passage of drugs (2,3). Once the molecule or drug crosses the stratum corneum and reaches the deeper layers of the skin, it can be absorbed systemically (4).

So, one of the strategies used to promote the transdermal passage of drugs is their nanoencapsulation. It has been shown that nanometer-sized systems can cross the skin and deliver drugs to deeper layers of it (5). For the promoting effect of the nanosystems to be maximized, they must have a size of less than 500 nm so that they penetrate the skin not only through the hair follicles but also through the stratum corneum (6,7). Although the ideal size is still unknown, it is believed that smaller systems penetrate the skin better (6,8,9).

In this study, the transdermal absorption of nanoencapsulated imiquimod was evaluated. Imiquimod is an immunomodulatory drug used topically for cell carcinoma, actinic keratosis and genital and perianal warts (10). However, some studies, using a commercial imiquimod cream have shown that its absorption was practically null

María Javiera Alvarez-Figueroa and José Vicente González-Aramúndiz contributed equally to this work.

✉ María Javiera Alvarez-Figueroa
mjalvare@uc.cl

✉ José Vicente González-Aramundiz
jvgonzal@uc.cl

[1] Facultad de Química y de Farmacia, Departamento de Farmacia, Pontificia Universidad Católica de Chile, Vicuña Mackena 4860, CP: 7820436 Macul, Santiago, Chile

[2] Laboratorio de Espectroscopia Vibracional, Facultad de Ciencias, Universidad de Chile, Santiago, Chile

[3] Centro de Investigación en Nanotecnología y Materiales Avanzados "CIEN-UC", Pontificia Universidad Católica de Chile, Santiago, Chile

and skin retention was very low (3–19%) (11,12). This can be explained by imiquimod's physicochemical properties: it is a hydrophobic molecule (log P: 3.0) and has poor solubility in water (18 μg/mL) or organic solvents (e.g. 96 μg/mL in acetone, 120 μg/mL in propylene glycol) (13). Therefore, designing a nanocarrier for imiquimod with special components could improve its properties. For example, imiquimod has a good solubility in fatty acids (14). Therefore, using linoleic acid as chitosan nanocapsules' constituent could help transport more drug. In addition, the use of an innovative excipient for the transdermal administration, such as Compritol 888 ATO®, could influence the kinetic delivery of imiquimod since this function has been demonstrated when it was incorporated as a lubricant or coating agent for oral solid dosage formulations (15). Nevertheless the potential of compritol in transdermal delivery has been largely unexplored. In transdermal studies compritol has been tested as an ingredient in solid lipid nanoparticles (SLN), where the transdermal enhancer action when compared to others lipids (e.g. glyceryl palmitostearate, Precirol® ATO 5) could be due to the increase of the solubility of the active pharmaceutical ingredient (terbinafine) (16). More recently, studies have shown that an increase of the amount of compritol in SLN showed an increase in transdermal absorption of triclosan. This could be because of the occlusive effect of compritol or other lipid contents over the skin (17).

In recent years, studies using Raman microscopy to evaluate the transdermal penetration of different molecules (caffeine, flufenamic acid, oxaprozin), have been published (18–21). This technique allows obtaining chemical and structural information of the skin, as well as the physical distribution of its constituents, with the advantage of it being a technique suitable for the analysis of biological aqueous samples (tissue) because no water signal interference occurs (22,23). In addition, it has the advantage of being a non-invasive method that does not require sample preparation (24). Thus, this technique can be used to analyse the skin's physiological components or to evaluate molecular kinetics of transdermal penetration (20,25–27). Raman spectroscopy analysis is based on the examination of the light scattered by a material when a monochromatic beam of light strikes it. A small portion of the light is inelastically dispersed, undergoing small changes in the frequency that is characteristic of the analysed material and therefore a characteristic chemical fingerprint is generated for this material (21,28).

In the present study, chitosan nanocapsules, using components that promote their transdermal penetration and modify their release, were designed. Raman microscopy was used to study whether these imiquimod loaded- chitosan nanocapsules were able to cross the stratum corneum (the skin layer that opposes the passage of molecules) and how their penetration kinetics was.

MATERIALS AND METHODS

Reagents

Potassium chloride, acetone, ethanol, methanol, sodium acetate, acetic acid, SDS and imiquimod were purchased from Merck (Germany). Poloxamer 188®, PEG-40 stearate®, ammonium acetate, phosphate buffered saline and linoleic acid were obtained from Sigma Aldrich (Germany). Formalin 37% and xylol were obtained from Coprolan LTDA (Chile), Chitosan HCl was purchased from Heppe Medical Chitosan GmbH (Germany). Paraffin Paraplast Plus was obtained from Leica Byosistems (Germany). Lipoid P75® and Compritol 888 ATO® were kindly donated by Lipoid (Germany) and Gattefossé (France) respectively.

Preparation of Chitosan Nanocapsules

Chitosan nanocapsules (Cs NCs) were made using the solvent displacement method (1,29). For the blank Cs NCs (without imiquimod), the organic phase consisted in linoleic acid (63 μL), PEG 40-stearate (7.5 mg) and lecithin (Lipoid P75®, 7.5 mg) dissolved in 0.5 mL of ethanol; and Compritol 888 ATO® (10 mg) dissolved in 5,0 mL of ethanol: acetone 1:18. The aqueous phase was 10 mL water with chitosan HCl (5 mg) and Poloxamer 188® (25 mg). The organic phase was added to the aqueous phase by pressure, using a syringe. For the complete evaporation of the organic solvents, the mixture of both phases was deposited in a rotary evaporator (Heidolph, Germany) until a final volume of 5 mL was obtained. For imiquimod- loaded chitosan nanocapsules (Cs NCs-Imq), 0.945 mg of this drug (Sartorius micro, Fisons instruments, Italy) was dissolved in the same quantity as linoleic acid. Centrifugation was used to isolate the Cs NCs (Universal 320 R, Hettich). For this, the sample was deposited in Amicon® (10,000 MCWO) centrifuge tubes. The conditions used were: 4000 RPM, 30 min, 4°C. The supernatant was resuspended in an equal volume of purified water (isolated Cs NCs-Imq).

Physicochemical Characterization (Size, Polydispersity Index and Zeta Potential)

The characterization of nanosystems was determined by measuring their physicochemical properties such as size and polydispersity index by Dynamic Light Scattering; and zeta potential (ζ potential) by laser-Doppler anenometry (NanoZS90 ® ®, Malvern Instruments, Malvern, UK) (30,31). To measure size, the samples were diluted in purified water, while to measure ζ potential, they were diluted in a 1 mM potassium chloride solution.

Encapsulation Efficiency of Imiquimod

Imiquimod was quantified using Ultra High-Performance Liquid Chromatography with a mass detector (UHPLC-MS/MS, EkspertTM ultraLC 100, Denaher Coporation, AB Sciex, SA). An Atlantis Silica HILIC Column (100 Å, 5 µm, 2.1 mm × 150 mm, Waters, USA) was used and the mobile phase consisted of 20% methanol and 80% aqueous 5 mM ammonium acetate, with a flow of 0.5 mL/min without a gradient. The total time of each chromatographic run was 4 min. The column was thermoregulated at 40°C and the samples at 15°C. The injection volume was 10 µL.

The ionization method was positive and the mass/load transitions that were analyzed were 241,014 to 185,000 and from 241,014 to 113,900 with collision energies of 13 V and 19 V respectively. The parameters were CUR: 20 Psi, IS: 3500 v, GS1: 50 Psi, GS2: 50 Psi, CAD: 9 v, DP: 86 v, EP: 10 v. Under this method, the retention time of imiquimod was 1 min.

For the quantification of imiquimod, a calibration curve was prepared each time the samples were analyzed. The concentrations of imiquimod used were 10, 20, 30, 40, 60 and 70 PPB, using methanol as solvent. An adequate curve was considered when the correlation coefficient r^2 was >0.99.

The encapsulation efficiency of imiquimod was determined by calculating the ratio between the imiquimod quantified in the isolated Cs NCs-Imq and the amount of this drug found in the non-isolated Cs NCs-Imq (see 2.2).

Nanocapsule Stability

The stability of the Cs NCs-Imq, under physiological (PBS pH 7.4, 37°C) and storage conditions (4°C) was evaluated. This study was carried out through their physicochemical characterization (size and polydispersity index) at different times. For physiological condition the schedule was 0.5, 1, 2, 4, 6, 24 and 48 h, and for storage conditions was 0.25, 0.50, 0.75, 1, 2 and 3 month. During the whole test the samples were protected from light ($n = 3$).

Freeze-Drying of Chitosan Nanocapsules

The Cs NCs-Imq were mixed with the same volume of milli Q water or with cryoprotectants. Glucose, sorbitol and mannitol at 5 and 10% *w/v* were tested as cryoprotectant. 1 mL of these mixtures 1:1 was frozen at −80°C overnight and then placed in the freeze dryer (FreeZone®, Labconco, United States). The process was at −50°C and a 0.1 mbar pressure. After 48 h, the samples were removed and stored in a desiccator at room temperature and covered with light. To measure the stability of the Cs NCs-Imq, the samples were resuspended in their initial volume (0.5 mL of mili Q water) at different times: day 1, week 1, 2, 4, 6 and 8; and their physicochemical parameters were determined (see 2.3). The study was carried out in triplicate ($n = 3$).

Imiquimod Release

The imiquimod release from the Cs NCs-Imq with and without Compritol 888 ATO® (control) was studied by quantifying the content of imiquimod released through UHPLC-MS/MS. For this, side by side diffusion cells (0.78 cm^2 area, PermeGear. Inc. USA) were used separated by a cellulose dialysis membrane (25 mm high, Sigma-Aldrich, Darmstadt, Germany). The donor was 0.175 mL of the isolated Cs NCs-Imq with 3.325 mL of acetate buffer pH 5.5 (imiquimod concentration of 0.189 mg/mL). The receptor solution was 3.5 mL of acetate buffer pH 5.5. The system was maintained at 37°C, under stirring and protected from light throughout the experiment. Samples of 2 mL of receptor solution were taken at different times; 1, 3, 5, 20 and 24 h, replenishing equal volumes of fresh solution for *sink* conditions were maintained throughout the experiment (32). Subsequently, these samples were diluted in order to be quantified according to the description in point 2.2.

Results are presented as mean ± SD ($n = 3$) and data were analysed by the unparaded student test ($p < 0.05$).

Raman Spectra

The Raman spectra were obtained using a MicroRaman (Witec alpha-300 RA, Confocal DT) a laser excitation source at 532 nm and a 20X or 50X oil immersion objective (20). The acquisition of the data was obtained by the Witec control software and the analysis and interpretation of the spectral information was carried out in Origin pro 2017 (20). The spectrum of each of the components of the Cs NCs- Imq (linoleic acid, Poloxamer 188®, PEG-40 stearate®, Lipoid P75®, Compritol 888 ATO®, chitosan HCl, imiquimod) and the Cs NCs-Imq after transdermal experiments (see below 2.8) was obtained. Each sample was placed on a slide (25.4 × 76.2 mm) in its physical state at room temperature, either liquid or solid. The conditions used to obtain these spectra were: step 6 or 30 and different integration time. (30s, 2 s or 60s). The skin and blank Cs NCs spectra were also obtained.

Transdermal Experiments

For these experiments, newborn pig skin was used (1,33,34), which was extracted and then stored at −20°C before use (35). The skin was cut to a suitable size and placed in Franz vertical diffusion cells (area 4.15 cm^2, Laboratory Glass Apparatus Inc., USA), so that the epidermis was in contact with the donor compartment. The system was kept at a constant temperature (37°C), under agitation and protected from light throughout the experiment. The donor solution consisted of

1 mL of the Cs NCs-Imq and the receptor solution of approximately 5 mL of acetate buffer pH 5.5. Throughout the experiment, the latter was under sink conditions. After 24 h the skin was removed and washed with methanol. Then, the skin Raman spectra were collected. The choice of the area to be measured was made by obtaining spectra from different sectors of the analyte and the point where most information was obtained.

Deepness of Imiquimod Transdermal Absorption Studied by Raman Spectroscopy

When the imiquimod transdermal experiment was finished (see 2.8), the skin was deposited 24 h in each of the following solvents: formalin 10% in PBS, ethanol 50%, ethanol 75%, ethanol 96%, ethanol 100% and Xilol. Finally, the skin was left in paraffin for 30 days. At the end of the month, a paraffin cube was formed with the skin inside. Then the skin was cut with a microtome (0.16 μm) and deposited over a slide using egg albumin. Subsequently, the paraffin was removed from the slide by submerging the sections in xylol for 10 min. The histological section was placed on the slide, moving the laser manually from the epidermis to the hypodermis (perpendicular on the surface of the skin) (36). These measurements were carried out at room temperature, using a 50X objective, 532 nm laser, 30 accumulations and integration time of 2 s.

Kinetic Evaluation of Imiquimod Transdermal Penetration by Raman Microscopy

A study was done as described in 2.8 using a Franz cell built and adapted to be placed on the microscope stage (area 4.15 cm^2). A point of the skin was chosen, at a depth greater than 20 μm to make sure that it had crossed the stratum corneum and was in the deeper layers of the skin (37), which was measured every 30 min for a total time of 6 h.

RESULTS AND DISCUSSION

In this study, chitosan nanocapsules for imiquimod transdermal administration were designed (Cs NCs-Imq) and their transdermal penetration was evaluated by Raman Microscopy.

The chitosan nanocapsules were prepared by solvent displacement method (38), a method that does not need great energy and generates nanosystems of reproducible size. A syringe was used to add the oil phase on the aqueous phase by pressure to obtain nanocapsules with smaller particle sizes (39) .

Some of the excipients used in the novel formulations were: a) Compritol® 888 ATO, a lipid composed of a mixture of different glycerol esters with behenic acid (C_{22} fatty acid) that has been used for modified-release tablets for oral administration (15,40) and which has also shown to be a transdermal enhancer (16,17); b) linolenic acid, a fatty acid that helps maintain the barrier function of the skin through maturation and differentiation of the stratum corneum (41) and which has been shown to help the healing of skin wounds (42); and c) chitosan, a cationic polysaccharide extracted from the shells of crustaceans composed of D-glucosamine and N-acetyl-D-glucosamine (43), with mucoadhesive properties, and capable of enhancing the transdermal passage of drugs since it opens the tight junctions (7). Starting materials used in our developed nanosystems are GRAS (Generally recognized as Safe) and should not present cytotoxicity.

Characterization and Stability of the Designed Nanosystems

The designed chitosan nanocapsules (see Table I) have a nanometric size (~ 200 nm) and the polydispersion index (PI) was always <0.3 (indicative of a single monomodal distribution in particle size) (44,45). **ζ** potential was positive; indicating that chitosan is arranged as a shell around the NCs-Imq nanodroplets (1,43). Also, this surface property was not alternating when imiquimod was incorporated into the chitosan nanocapsules. The encapsulation efficacy was 73%, similar to values reported for nanoencapsulation of other active ingredients (1).

Additionally, imiquimod-loaded chitosan nanocapsules (Cs NCs-Imq) proved to be stable for at least 48 h in physiological condition since their particle size and PI practically did not change in this condition (pH 7.4, 37°C,). However, under storage conditions (4°C) at 2 weeks the particle size increased by two-fold and PI >0.3. This increase in diameter after storage condition has also been observed by other authors who have studied solid lipid nanoparticles with Compritol® 888 ATO, suggesting that there could be a certain degree of particle flocculation under these conditions (46).

It was then studied whether the lyophilization process could increase Cs NCs-Imq stability since it is known that this form of drying improves the long-term stability of colloidal nanoparticles (47,48). Figure 1 shows the physicochemical properties of the Cs NCs-Imq after their freezing, studying the dilution effect and the use of different cryoprotectants.

Firstly, it was observed that Cs NCs-Imq diluted in water (1:1) lose their physicochemical properties and aggregation can be seen, which shows the need to use cryoprotectants. It was observed that when glucose or mannitol was used, an increase in their respective concentrations caused an increase in the size of the chitosan nanocapsules, without causing a greater variation in the zeta potential. In the case of glucose, there are several studies that report what has been observed. For example, Sameti et al. report that when increasing glucose from 5% to 10–20% to lyophilize cationic silica nanoparticles, the particle size increased 2 to 4 times (49). This could be

Table I Physicochemical Properties of Blank Chitosan Nanocapsules (Cs NCs) and Imiquimod-Loaded Chitosan Nanocapsules (Cs NCs-Imq). PI: Polydispersion Index. Mean ± S.D. ($n \geq 3$)

Nanosystem	Size (nm)	PI	ζ Potential (mv)	Encapsulation efficacy (%)
Cs NCs	226 ± 22	0.175	+16 ± 1	
Cs NCs-Imq	180 ± 17	0.178	+17 ± 2	73 ± 4

explained by the affinity through hydrogen bonds between glucose and Poloxamer 188®, which causes these nanosystems to increase in size when resuspended, with this increase directly proportional to the glucose concentration (47). Regarding mannitol, it was also observed that PI increased when increasing the concentration of this sugar. This could be due to its glass transition temperature that would prevent its crystallization in an amorphous way (50); since one of the proposed mechanisms in the lyophilization stabilization process, is that the cyoprotectant forms an amorphous crystal that protects the formulation from the stress of the water when sublimating (51). The case of sorbitol was different because the chitosan nanocapsules maintained their properties at the highest concentration of this sugar (10%). To continue with the studies of the stability of lyophilized chitosan nanocapsules over time, 5% glucose was chosen as a cryoprotectant, because it has been reported that it is a more efficient cryoprotectant than sorbitol to stabilize nanosystems that incorporate a hydrophobic molecule, as is the case of the designed chitosan nanocapsules (Cs NCs-Imq) (52).

Figure 2 shows the stability of freeze-drying chitosan nanocapsules over time using 5% glucose. It is observed that the Cs NCs-Imq size increased around 60 nm when they are lyophilized, but they maintained their nanometric properties for at least 2 months (and PI <0.3). Furthermore, **ζ** potential remained positive during that time, indicating that the chitosan shell remains in the nanosystems after the freeze dried process.

With these results it is verified that the designed chitosan nanocapsules, which contain novel excipients (Compritol® 888 ATO, linoleic acid and chitosan) have the optimal size to be administered through the skin (<500 nm) and that they are stable for 48 h under physiological conditions and for at least 2 months when they are lyophilized. Therefore, Cs NCs-Imq have the adequate physical chemical properties to be used as an imiquimod transdermal vehicle.

Imiquimod Release Profile

These studies were done to verify that the controlled release properties attributable to Compritol® 888 ATO in solid pharmaceutical forms are maintained when used as an excipient to formulate transdermal chitosan nanocapsules. Imiquimod release profiles from Cs NCs-Imq with and without Compritol® 888 ATO (control) are shown in Fig. 3. It is observed that Compritol® 888 ATO influences imiquimod's release. Specifically, at 24 h the Cs NCs-Imq without Compritol® 888 deliver twice this drug in comparison with control ($p < 0.05$). This shows that the Cs NCs-Imq components were adequate to observe the controled release effect of Compritol® 888 ATO. This is consistent with what has been reported by other authors, which has shown that the components of the formulations have a great influence on matrix formation and drug release from Compritol® 888 ATO - based matrix (40).

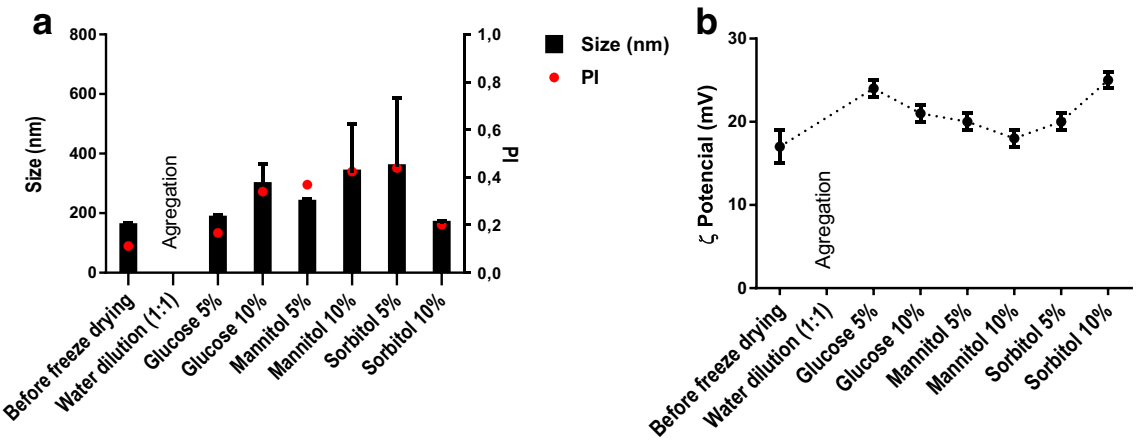

Fig. 1 Effect of cryoprotectants on imiquimod-loaded chitosan nanocapsule stability by freeze-drying. (**a**) Particle size (nm) and polydispersion index (PI). (**b**) ζ Potential. Mean ± S.D. ($n = 3$).

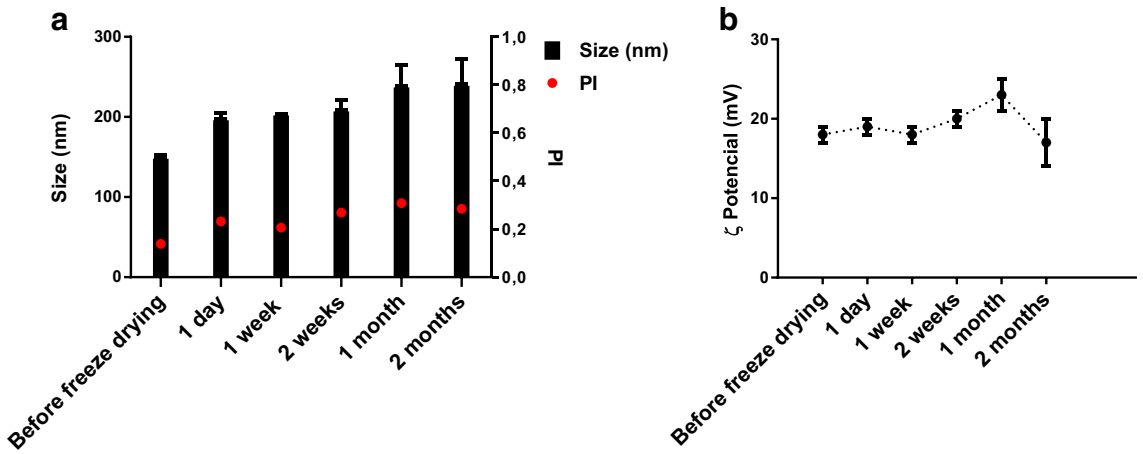

Fig. 2 Stability of freeze-drying chitosan nanocapsules over time. (**a**) Particle size (nm) and polydispersion index (PI). (**b**) ζ Potential. Cryoprotectant: 5% glucose. Mean ± S.D. (n = 3).

Transdermal Experiments by Raman Microscopy

In the transdermal penetration studies, newborn pig skin was used, as it is similar to human skin in hair follicle density, lipophilic composition and blood vessel distribution (34).

Figure 4 shows the Raman spectra obtained for each imiquimod-loaded chitosan nanocapsule component and the Cs NCs-Imq. All these spectra were compared with those described in the bibliography (53,54). Analysing some spectra it was observed that: a) For Compritol 888 ATO® the spectrum has characteristic bands of vibrations of C-C groups (aliphatic chains) between 1080 and 1293 cm^{-1}, groups CH_2 and CH_3 in 1438 cm^{-1}, 2846 cm^{-1} and 2879 cm^{-1}; it is not possible to distinguish bands from ester or OH groups, possibly because the relative intensity of the vibrational modes is lower compared to other more active modes in Raman (54). b) For imiquimod the following was observed: the characteristic deformation bands of the aliphatic chains between 467 and 876 cm^{-1}, the band of the isopropyl group at 1368 cm^{-1}, bands of the aromatic rings between 990 and 1034 cm^{-1} (54), the C-NH_2 band in 1333 cm^{-1}, the band of groups CH_2 and CH_3 between 1400 and 1496 cm^{-1}, the band of heterocycles in 1618 cm^{-1}, the band of C = C in 3078 cm^{-1} and the NH_2 group band at 3175 cm^{-1} (54). c) For linoleic acid the spectrum was similar to that reported (54); bands at 844, 914, 977, 1084, 1261 and 1300 cm^{-1} corresponding to C-C are observed, the band of 1445 cm^{-1} assigned to coupled deformations of CH_2 and CH_3, the band 1654 cm^{-1} attributed to streaching C = C and COOH. Finally, bands at 2729, 2852 and 2903 cm-1 are assigned to vCH of the aliphatic CH_2 and the band at 3017 cm-1 contains information of OH and CH stretching modes.

The Raman spectrum of the skin used as a model in this study was also obtained (see Fig. 5**)**, with the observation that

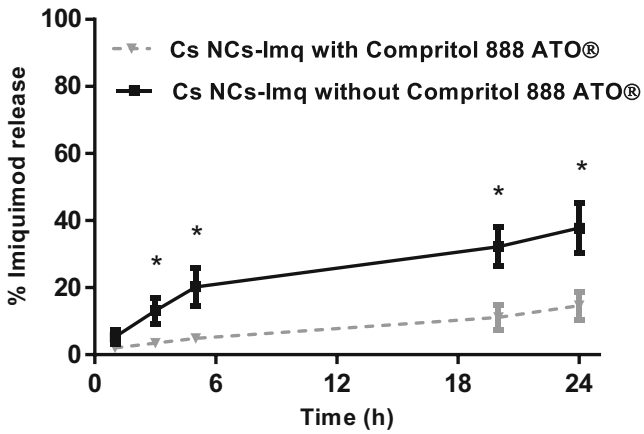

Fig. 3 Imiquimod-loaded chitosan nanocapsule release profile. Mean ± S.D. (n = 3). * Statistically significant $p < 0.05$.

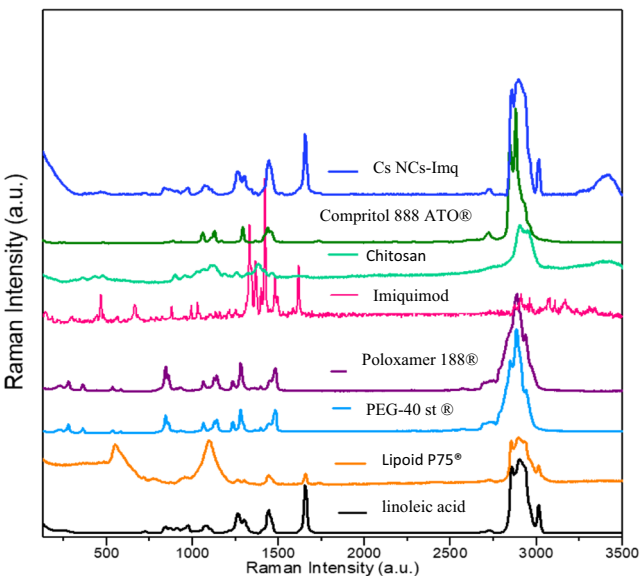

Fig. 4 Raman spectra of each imiquimod-loaded chitosan nanocapsules (Cs NCs-Imq) component and the Cs NCs-Imq.

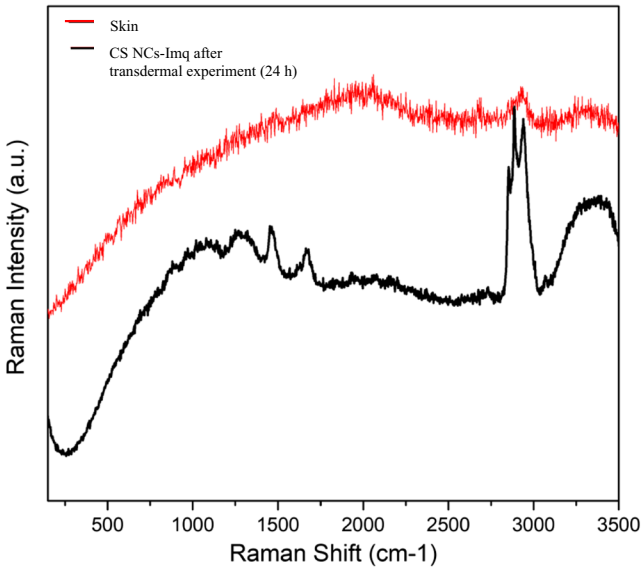

Fig. 5 Raman spectra of skin and imiquimod-loaded chitosan nanocapsules (Cs NCs-Imq) after transdermal experiments (24 h).

it presents fluorescence and a single band at 2924 cm-1, which corresponds to aliphatic vibrations (25,55). Subsequently, the Cs NCs-Imq spectra after transdermal experiments were obtained (see Fig. 5**)**, observing bands absent in the skin-only spectrum. Analysing all this information, it was not possible to identify a single characteristic band for Cs NCs-Imq. Regarding this, Jamieson et al. (56) indicate that in order to understand subtle changes in the Raman spectra when biological samples are used, the Raman spectrum should not be considered as the result of the sum of all the compounds observed there. Therefore, more than a band-by-band analysis, trends within the spectrum must be identified. For this reason, it was decided to evaluate the imiquimod transdermal penetration by general spectra and not for a specific band.

Deepness of Imiquimod Transdermal Absorption by Raman

The Raman spectra obtained for the skin (histological sections) after 24 h in contact with Cs NCs-Imq are shown in Fig. 6. It is observed that the imiquimod bands are seen at depths greater than 20 μm (37,57), that is, the drug has already crossed the stratum corneum and it is found in deeper layers of the skin, therefore it is available to be absorbed (4). With these results, it is verified that Cs NCs-Imq transdermal penetration can be studied using Raman microscopy and it is possible to use this technique to know in which skin layer it is found. This study demonstrates that Raman microscopy is an alternative to determine the drug absorption in different layers of the skin and it is less cumbersome to do so in comparison to other methods, such as the case of microtome (13,58) or tape stripping (12,14,59).

Kinetic Evaluation of Imiquimod Transdermal Penetration by Raman

The Raman spectra of the kinetic study of Cs NCs-Imq transdermal penetration for 6 h are shown in the Fig. 7. It is observed that the process of penetration through the skin is dynamic. It is also observed that Cs NCs-Imq penetrate the stratum corneum quickly (approximately 50 min), are present in the skin approximately for 4 h and then tend to decrease. One of the components of NCs-Imq is chitosan, which was

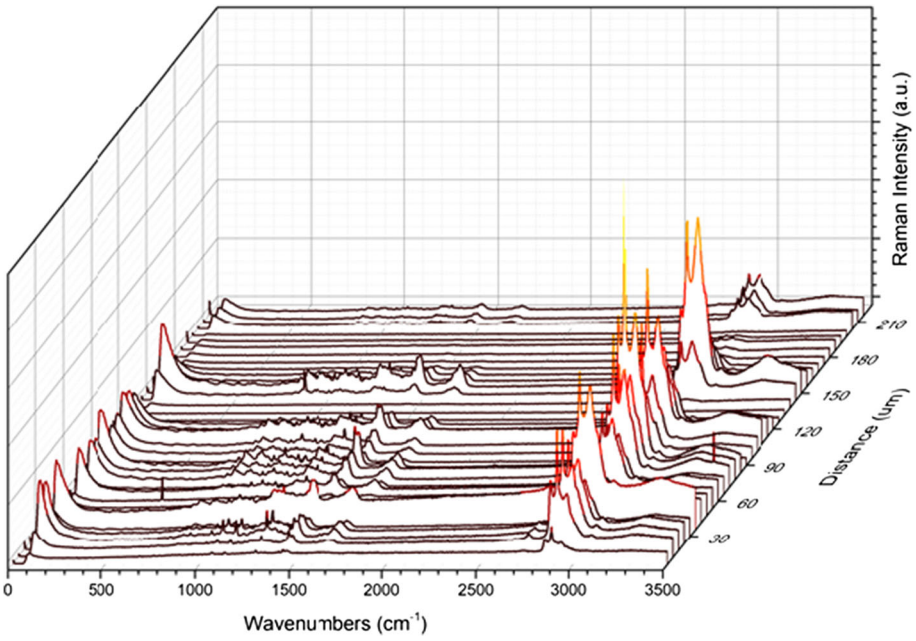

Fig. 6 Transdermal penetration of imiquimod-loaded chitosan nanocapsules after 24 h: evaluation by Raman.

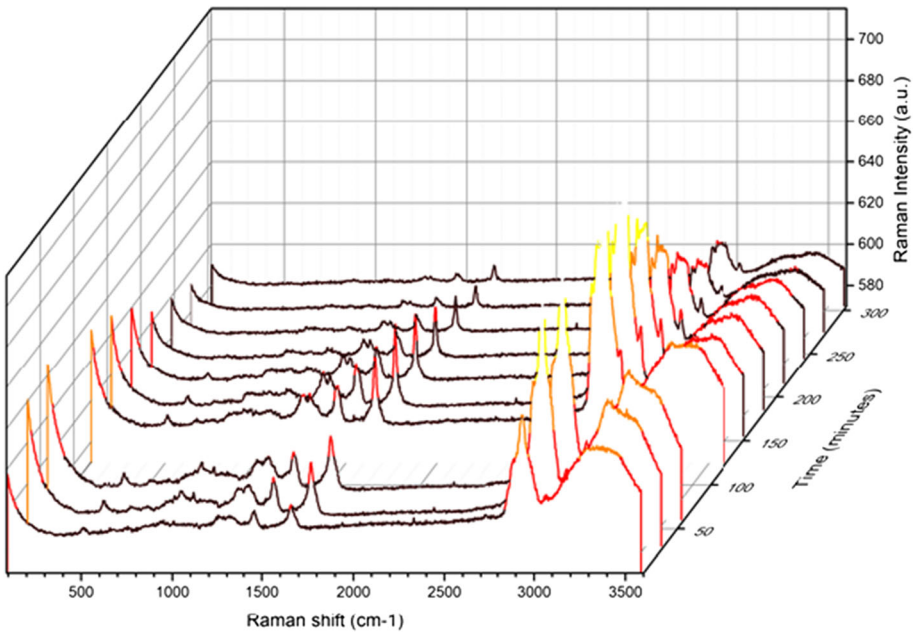

Fig. 7 Kinetic transdermal penetration of imiquimod-loaded chitosan nanocapsules, evaluation by Raman spectroscopy.

chosen as a polymeric cover giving a positive charge to nanocapsules. Positively charged nanocapsules were designed because the residual amino acids of the skin at physiological pH have a negative charge, and it is expected to find a greater transdermal transport of cations than of anions (60–62).

This study demonstrates that Raman microscopy is suitable for studying the nanovehicles transdermal penetration. More specifically, through Raman microscopy we demonstrate that Cs NCs-Imq penetrate the stratum cornea and are available to be absorbed.

CONCLUSIONS

In the present work, the chitosan nanocapsules designed for imiquimod transdermal administration had nanometric size (180 nm), a monomodal distribution in particle size, high encapsulation, good stability for at least 48 h in physiological conditions and they maintained their physicochemical properties after 2 months when they were lyophilized. The effect of Compritol® 888 ATO in the imiquimod control release was observed. Using Raman microscopy, it was demonstrated that the designed imiquimod-loaded chitosan nanocapsules penetrate the skin dynamically and that it takes at least 50 min to pass the stratum corneum.

Acknowledgements and Disclosures. This work was supported by Fondo Nacional de Desarrollo Científico y Tecnológico de Chile (FONDECYT 1201482 to J.V. González-Aramundiz) and Programa de Equipamiento Científico y Tecnológico (FONDEQUIP EQM120021 and FONDEQUIP EQM130032).

REFERENCES

1. Alvarez-Figueroa MJ, Abarca-Riquelme JM, González-Aramundiz JV. Influence of protamine shell on nanoemulsions as a carrier for cyclosporine-a skin delivery. Pharm Dev Technol. 2019;24(5):630–8.
2. Wiedersberg S, Guy RH. Transdermal drug delivery: 30+ years of war and still fighting! J Control Release. 2014;190:150–6.
3. Münch S, Wohlrab J, Neubert RHH. Dermal and transdermal delivery of pharmaceutically relevant macromolecules. Eur J Pharm Biopharm. 2017;119:235–42.
4. Guy RH. Transdermal drug delivery. In: Schäfer-Korting M, editor. Drug Delivery. Berlin, Heidelberg: Springer Berlin Heidelberg; 2010. p. 399–410.
5. Pegoraro C, MacNeil S, Battaglia G. Transdermal drug delivery: from micro to nano. Nanoscale. 2012;4(6):1881–94.
6. Su R, Fan W, Yu Q, Dong X, Qi J, Zhu Q, et al. Size-dependent penetration of nanoemulsions into epidermis and hair follicles: implications for transdermal delivery and immunization. Oncotarget. 2017;8(24):38214–26.
7. Bussio J, Molina-Perea C, González-Aramundiz J. Lower-sized chitosan Nanocapsules for transcutaneous antigen delivery. Nanomaterials. 2018;8(9):659.
8. Gupta R, Rai B. Effect of size and surface charge of gold nanoparticles on their skin permeability: a molecular dynamics study. Sci Rep. 2017;7:45292.
9. Howard GP, Verma G, Ke X, Thayer WM, Hamerly T, Baxter VK, et al. Critical size limit of biodegradable nanoparticles for enhanced lymph node trafficking and paracortex penetration. Nano Res. 2019;12(4):837–44.
10. Hanna E, Abadi R, Abbas O. Imiquimod in dermatology: an overview. Int J Dermatol. 2016;55(8):831–44.
11. Stein P, Gogoll K, Tenzer S, Schild H, Stevanovic S, Langguth P, et al. Efficacy of imiquimod-based transcutaneous immunization using a nano-dispersed emulsion gel formulation. PLoS ONE. 2014;9(7):e102664-e.
12. Al-Mayahy MH, Sabri AH, Rutland CS, Holmes A, McKenna J, Marlow M, et al. Insight into imiquimod skin permeation and increased delivery using microneedle pre-treatment. Eur J Pharm Biopharm. 2019;139:33–43.

13. Lapteva M, Mignot M, Mondon K, Möller M, Gurny R, Kalia YN. Self-assembled mPEG-hexPLA polymeric nanocarriers for the targeted cutaneous delivery of imiquimod. Eur J Pharm Biopharm. 2019;142:553–62.
14. Pescina S, Garrastazu G, del Favero E, Rondelli V, Cantù L, Padula C, et al. Microemulsions based on TPGS and isostearic acid for imiquimod formulation and skin delivery. Eur J Pharm Sci. 2018;125:223–31.
15. Aburahma MH, Badr-Eldin SM. Compritol 888 ATO: a multi-functional lipid excipient in drug delivery systems and nanopharmaceuticals. Expert Opin Drug Deliv. 2014;11(12):1865–83.
16. Chen Y-C, Liu D-Z, Liu J-J, Chang T-W, Ho H-O, Sheu M-T. Development of terbinafine solid lipid nanoparticles as a topical delivery system. Int J Nanomedicine. 2012;7:4409–18 Epub 2012/08/15.
17. Kakadia PG, Conway BR. Solid lipid nanoparticles for targeted delivery of triclosan into skin for infection prevention. J Microencapsul. 2018;35(7–8):695–704.
18. Franzen L, Selzer D, Fluhr JW, Schaefer UF, Windbergs M. Towards drug quantification in human skin with confocal Raman microscopy. Eur J Pharm Biopharm. 2013;84(2):437–44.
19. Uragami C, Yamashita E, Gall A, Robert B, Hashimoto H. Application of resonance raman microscopy to in vivo carotenoid. Acta Biochim Pol. 2012;59(1):53–6.
20. Pyatski Y, Zhang Q, Mendelsohn R, Flach CR. Effects of permeation enhancers on flufenamic acid delivery in ex vivo human skin by confocal Raman microscopy. Int J Pharm. 2016;505(1):319–28.
21. Liu S, Bao X, Zhang S, Zhang H, Lu X. Li T, et al. Drug Deliv Transl Res: The study of ultrasound and iontophoresis on oxaprozin transdermal penetration using surface-enhanced Raman spectroscopy; 2019.
22. Darlenski R, Fluhr JW. In vivo Raman confocal spectroscopy in the investigation of the skin barrier. Curr Probl Dermatol. 2016;49:71–9.
23. Ali SM, Bonnier F, Lambkin H, Flynn K, McDonagh V, Healy C, et al. A comparison of Raman, FTIR and ATR-FTIR micro spectroscopy for imaging human skin tissue sections. Anal Methods. 2013;5(9):2281–91.
24. Caspers PJ, Bruining HA, Puppels GJ, Lucassen GW, Carter EA. In vivo confocal Raman microspectroscopy of the skin: noninvasive determination of molecular concentration profiles. J Invest Dermatol. 2001;116(3):434–42.
25. Franzen L, Windbergs M. Applications of Raman spectroscopy in skin research — from skin physiology and diagnosis up to risk assessment and dermal drug delivery. Adv Drug Deliv Rev. 2015;89:91–104.
26. Atef E, Altuwaijri N. Using Raman spectroscopy in studying the effect of propylene glycol, oleic acid, and their combination on the rat skin. AAPS PharmSciTech. 2018;19(1):114–22.
27. Mujica Ascencio S, Choe C, Meinke MC, Müller RH, Maksimov GV, Wigger-Alberti W, et al. Confocal Raman microscopy and multivariate statistical analysis for determination of different penetration abilities of caffeine and propylene glycol applied simultaneously in a mixture on porcine skin ex vivo. Eur J Pharm Biopharm. 2016;104:51–8.
28. Vanden-Hehir S, Tipping WJ, Lee M, Brunton VG, Williams A, Hulme AN. Raman imaging of Nanocarriers for drug delivery. Nanomaterials (Basel). 2019;9(3):341.
29. Tan TB, Yussof NS, Abas F, Mirhosseini H, Nehdi IA, Tan CP. Forming a lutein nanodispersion via solvent displacement method: the effects of processing parameters and emulsifiers with different stabilizing mechanisms. Food Chem. 2016;194:416–23.
30. Hassan PA, Rana S, Verma G. Making sense of Brownian motion: colloid characterization by dynamic light scattering. Langmuir. 2015;31(1):3–12.
31. Bhattacharjee S. DLS and zeta potential – what they are and what they are not? J Control Release. 2016;235:337–51.
32. Nothnagel L, Wacker MG. How to measure release from nanosized carriers? Eur J Pharm Sci. 2018;120:199–211.
33. Alvarez-Figueroa MJ, Muggli-Galaz C, González PM. Effect of the aggregation state of bile salts on their transdermal absorption enhancing properties. J Drug Deliv Sci Technol. 2019;54:101333.
34. Abd E, Yousef SA, Pastore MN, Telaprolu K, Mohammed YH, Namjoshi S, et al. Skin models for the testing of transdermal drugs. Clin Pharmacol. 2016;8:163–76.
35. Flaten GE, Palac Z, Engesland A, Filipović-Grčić J, Vanić Ž, Škalko-Basnet N. In vitro skin models as a tool in optimization of drug formulation. Eur J Pharm Sci. 2015;75:10–24.
36. Essendoubi M, Gobinet C, Reynaud R, Angiboust JF, Manfait M, Piot O. Human skin penetration of hyaluronic acid of different molecular weights as probed by Raman spectroscopy. Skin Res Technol. 2016;22(1):55–62.
37. Todo H. Transdermal permeation of drugs in various animal species. Pharmaceutics. 2017;9(3):33.
38. Jeevanandam J, Chan YS, Danquah MK. Nano-formulations of drugs: Recent developments, impact and challenges. Biochimie. 2016;128–129:99–112.
39. Crecente-Campo J, Alonso MJ. Engineering, on-demand manufacturing, and scaling-up of polymeric nanocapsules. Bioeng Transl Med. 2019;4(1):38–50.
40. Roberts M, Pulcini L, Mostafa S, Cuppok-Rosiaux Y, Marchaud D. Preparation and characterization of Compritol 888 ATO matrix tablets for the sustained release of diclofenac sodium. Pharm Dev Technol. 2015;20(4):507–12.
41. Huang T-H, Wang P-W, Yang S-C, Chou W-L, Fang J-Y. Cosmetic and therapeutic applications of fish Oil's fatty acids on the skin. Mar Drugs. 2018;16(8):256.
42. Pereira LA, Hatanaka E, Martins EF, Oliveira F, Liberti EA, Farsky SH, et al. Effect of oleic and linoleic acids on the inflammatory phase of wound healing in rats. Cell Biochem Funct. 2008;26(2):197–204.
43. Seferian PG, Martinez ML. Immune stimulating activity of two new chitosan containing adjuvant formulations. Vaccine. 2000;19(6):661–8.
44. Koroleva M, Nagovitsina T, Yurtov E. Nanoemulsions stabilized by non-ionic surfactants: stability and degradation mechanisms. Phys Chem Chem Phys. 2018;20(15):10369–77.
45. Wang Y, Zheng Y, Zhang L, Wang Q, Zhang D. Stability of nanosuspensions in drug delivery. J Control Release. 2013;172(3):1126–41.
46. Kuo Y-C, Chung C-Y. Solid lipid nanoparticles comprising internal Compritol 888 ATO, tripalmitin and cacao butter for encapsulating and releasing stavudine, delavirdine and saquinavir. Colloids Surf B Biointerfaces. 2011;88(2):682–90.
47. Abdelwahed W, Degobert G, Stainmesse S, Fessi H. Freeze-drying of nanoparticles: formulation, process and storage considerations. Adv Drug Deliv Rev. 2006;58(15):1688–713.
48. Hu Y, Ma C, Sun M, Guo C, Shen J, Wang J, et al. Preparation and characterization of nano amitriptyline hydrochloride particles by spray freeze drying. Nanomedicine. 2019;14(12):1521–31.
49. Sameti M, Bohr G, Ravi Kumar MNV, Kneuer C, Bakowsky U, Nacken M, et al. Stabilisation by freeze-drying of cationically modified silica nanoparticles for gene delivery. Int J Pharm. 2003;266(1):51–60.
50. Mensink MA, Frijlink HW, van der Voort MK, Hinrichs WLJ. How sugars protect proteins in the solid state and during drying (review): mechanisms of stabilization in relation to stress conditions. Eur J Pharm Biopharm. 2017;114:288–95.
51. Fonte P, Reis S, Sarmento B. Facts and evidences on the lyophilization of polymeric nanoparticles for drug delivery. J Control Release. 2016;225:75–86.

52. Yue P-F, Li G, Dan J-X, Wu Z-F, Wang C-H, Zhu W-F, et al. Study on formability of solid nanosuspensions during solidification: II novel roles of freezing stress and cryoprotectant property. Int J Pharm. 2014;475(1):35–48.
53. Scoutaris N, Vithani K, Slipper I, Chowdhry B, Douroumis D. SEM/EDX and confocal Raman microscopy as complementary tools for the characterization of pharmaceutical tablets. Int J Pharm. 2014;470(1):88–98.
54. Lin-Vien D, Colthup NB, Fateley WG, Grasselli In: Lin-Vien D, Colthup NB, Fateley WG, Grasselli JG, editors. The Handbook of Infrared and Raman Characteristic Frequencies of Organic Molecules. San Diego: Academic Press; 1991. p. 45–60.
55. Sdobnov AY, Tuchin VV, Lademann J, Darvin ME. Confocal Raman microscopy supported by optical clearing treatment of the skin-influence on collagen hydration. J Phys D Appl Phys. 2017;50(28).
56. Jamieson LE, Li A, Faulds K, Graham D. Ratiometric analysis using Raman spectroscopy as a powerful predictor of structural properties of fatty acids. Royal Society open science. 2018;5(12): 181483-.
57. Kitaoka M, Wakabayashi R, Kamiya N, Goto M. Solid-in-oil nanodispersions for transdermal drug delivery systems. Biotechnol J. 2016;11(11):1375–85. Epub 08/16.
58. Tessema EN, Gebre-Mariam T, Paulos G, Wohlrab J, Neubert RHH. Delivery of oat-derived phytoceramides into the stratum corneum of the skin using nanocarriers: formulation, characterization and in vitro and ex-vivo penetration studies. Eur J Pharm Biopharm. 2018;127:260–9.
59. Diblíková D, Kopečná M, Školová B, Krečmerová M, Roh J, Hrabálek A, et al. Transdermal delivery and cutaneous targeting of antivirals using a penetration enhancer and Lysolipid Prodrugs. Pharm Res. 2014;31(4):1071–81.
60. Abdel-Mottaleb MMA, Moulari B, Beduneau A, Pellequer Y, Lamprecht A. Surface-charge-dependent nanoparticles accumulation in inflamed skin. J Pharm Sci. 2012;101(11):4231–9.
61. Wu X, Landfester K, Musyanovych A, Guy RH. Disposition of charged nanoparticles after their topical application to the skin. Skin Pharmacol Physiol. 2010;23(3):117–23.
62. Dragicevic-Curic N, Gräfe S, Gitter B, Winter S, Fahr A. Surface charged temoporfin-loaded flexible vesicles: in vitro skin penetration studies and stability. Int J Pharm. 2010;384(1):100–8.